2015 IEEE-RAS 15th International Conference on Humanoid Robots (Humanoids)
November 3 - 5, 2015, Seoul, Korea

Human-Supervised Control of the ATLAS Humanoid Robot for Traversing Doors

Nandan Banerjee[1], Xianchao Long[1], Ruixiang Du[1], Felipe Polido[2], Siyuan Feng[2], Christopher G. Atkeson[2], Michael Gennert[1], and Taskin Padir[1]

***Abstract*— Door traversal is generally a trivial task for human beings but particularly challenging for humanoid robots. This paper describes a holistic approach for a full-sized humanoid robot to traverse through a door in an outdoor semi-structured environment as specified by the requirements of the DARPA Robotics Challenge. Door traversal can be broken down into four sub-tasks; door detection, walk to the door, door opening, and walk through the door. These topics are covered in detail along with the approaches used for perception and motion planning. Results from lab tests and the DRC Finals are shown. The approach presented in this paper can be further extended to a wide range of door types and configurations.**

I. Introduction

The DARPA Robotics Challenge (DRC) was aimed at advancing robotic technologies to assist humans in responding to natural and man-made disasters [1]. These systems had to be highly adaptable in order to robustly operate in unstructured and possibly chaotic environments. They had to handle severe communication degradation, and also needed to be able to manipulate their environment to accomplish critical goals.

This paper presents Team WPI-CMU's approach to performing the door task in the DRC Finals with the Boston Dynamics' Atlas humanoid robot. Atlas has 30 Degrees of Freedom (DoF), weighs approximately 180Kg, and stands tall at 1.80 meters (Fig. 1). Its lower limbs, torso and upper arms are composed of hydraulic joints, while the forearms and wrists are electrically powered. Our robot, WARNER(WPI's Atlas Robot for Non-conventional Emergency Response), is equipped with two Robotiq 3-finger hands as end-effectors, and it has a Carnegie Robotics' Multisense SL featuring a stereo camera and a spinning Hokuyo UTM-30LX-EW LIDAR for perception. Lastly, the robot also includes a battery system and wireless communication to operate without a tether. Additionally, there was no safety belay during the DRC Finals. Beyond the physical hardware, for offline and parallel testing, the use of a simulation environment in Gazebo was utilized.

Based on the DRC specifications, the robots are required to traverse a standard door with dimensions of 36 x 82 inches. It is assumed that the door has a lever handle and it has no significant deformations or holes, i.e., the door is solid. Moreover, the door can be left-handed or right-handed and can be opened by either pulling or pushing.

*N. Banerjee and X. Long contributed equally to this work
[1]Robotics Engineering, Worcester Polytechnic Institute
[2]Robotics Institute, Carnegie Mellon University

Fig. 1: The upgraded Atlas Humanoid Robot built by Boston Dynamics.

The door traversal problem for robots has been the focus of many research studies. Initially, researchers mainly approached this problem with wheeled robots [2] [3] [4]. However, for wheeled robots the interaction forces between the robot and the door have much less influence as the platforms are statically stable. Only in the last few years have researchers started to tackle door traversal using humanoid robots. Proposed methods include using a systematic touch scheme to grasp and turn the door knob [5], combining vision and tactile sensing to open the door [6], and stabilizing the robot against the reactive force of a door [7]. These methods provide insights into the door traversal problem in the lab environment but do not account for the wide range of conditions in an outdoor environment. The unpredictable outdoor conditions pose new challenges to the algorithms which work well in the lab. For example, many teams in the DRC Trials, including us, were influenced by the strong winds which blew the door shut after the robot opened it [8] [9] [10] [11] [12].

In this paper, we propose a method for robust humanoid door traversal that accounts for door detection in an outdoor unstructured environment, and high DoF motion planning. The paper is organized as follows: In Section II, we introduce our approach to humanoid door traversal. In Section III, we present how the main perception problem of door detection is addressed with both an automatic method and an operator-aided method. In Section IV, we describe the motion planning technique for WARNER to perform DRC manipulation tasks. In Section V, we show the performance of our methods. Lastly, Section VI concludes our presented work and discusses possible areas for future research.

978-1-4799-6885-5/15/$31.00 ©2015 IEEE

II. Approach

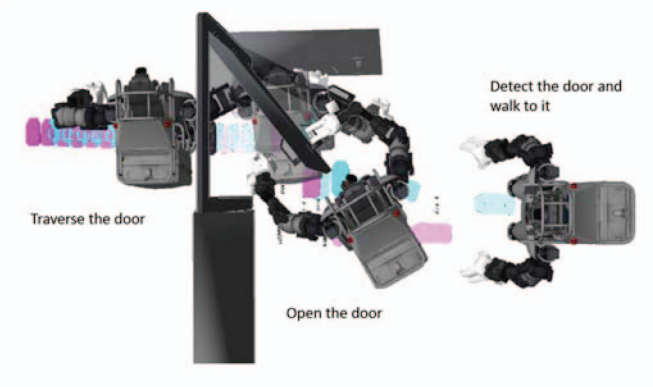

Fig. 2: Door Task Strategy

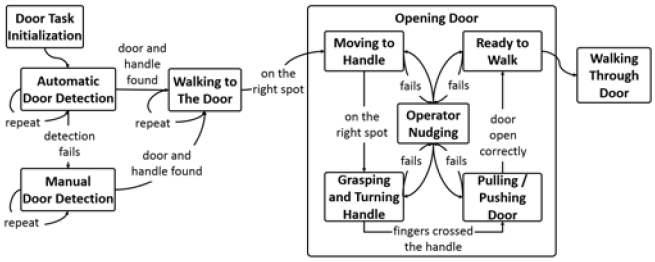

Fig. 3: Door task Finite State Machine

Our approach to traversing a right-handed pull door is illustrated in Fig. 2. The robot detects the door and door handle, approaches the door to position itself for holding the handle, opens the door by grasping and turning the handle, blocks the door by inserting the left arm, plans the steps and finally executes the door traversal. The footsteps generated by the step planned are also shown in Fig. 2. An event driven Finite State Machine(FSM) with the sub-tasks as the states is used to control the autonomous execution of the process with human validation at critical transitions (see Fig. 3). The FSM starts at the ***door detection*** state. Detection is performed using a vision based approach introduced in Section III. Once the robot has the normal to the door and the position of the handle, FSM transitions to the ***walking to the door*** state.

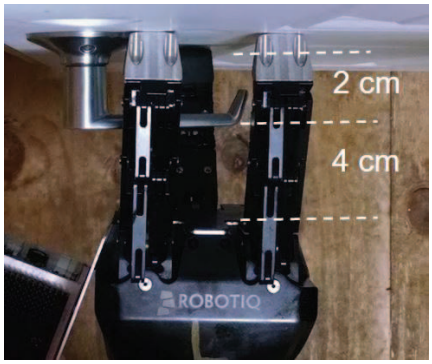

Fig. 4: Hand placement on door handle

At this point the robot follows a stepping trajectory generated by an A^* planner and walks to the desired stand position for opening the door. The third state in the FSM is ***opening the door***, which consists of four sub-states. First is ***moving to the handle***. Because of the dimension of the hand and the handle (see Fig. 4), the error that can be allowed between the desired hand position and the actual position is experimentally determined to be less than 2 cm. The second sub-state is ***grasping the handle***. Fig. 4 shows the position where the hand is ready to grasp. When the fingers touch the door, there is still sufficient space between the handle and the palm, which means the hand would generate an unexpected pulling force on the handle after fully grasping the handle. Therefore, the hand needs to move forward around 4 cm when applying the grasp motion. Third is ***opening the door***. In this state, our motion planning system is used to generate a sequence of motions, such as turning the handle, pulling out the door for the pull door (see Fig. 2) or pushing away the door for the push door, and raising the arm to prevent the door from closing. The details of generating these motions is described in Section IV. In the last sub-state, ***ready to walk***, the robot moves to the predefined pose for passing through the door. In case the robot does not move as expected in any of these sub-states, the operator can choose to repeat the state or pause and manually control the robot. The next state in the FSM is ***walking through the door***. The path planner, using a dynamic artificial potential field, generates an optimal step trajectory to pass through the door while the door can close by itself [13]. Due to the size of the Atlas robot with respect to the door size, the space available between the robot body and the door frame is sufficiently narrow to drastically limit the number of feasible trajectories for passing through the door.

III. Perception - Door Detection

Door detection in an unstructured outdoor environment can be a difficult problem, especially due to the ever changing lighting conditions. Many researchers have addressed the problem of door detection; Rusu [14] explored a way in which the doors can be detected in a point cloud using plane detection techniques alone. In contrast, Sekkal et al [15] used monocular vision to detect doors after segmenting out corridors in a given 2D scene. Shi et al [16] investigated detecting doors based on the inherent low level geometric features and their close relationship with corridors using a hypothesis generation and verification using a feedback method. A probabilistic framework modeling shape, color and the motion properties of a door and its surrounding objects fed through an Expectation-Maximization algorithm was extensively studied and implemented in a real world scenario at Stanford by Koller et al [17].

Due to the critical need of achieving reliable door detection for the DRC we developed two approaches in parallel; a fully automatic door detection algorithm, and a door detection algorithm that uses an operator input as seed.

A. Automatic door detection

The following assumptions are made. First, it is assumed that the distance, as obtained from the disparity map for any point on the door, is less than 5cm from the door plane. Second, the color of the handle should be significantly

Fig. 5: First row shows detected doors at various perspectives. Second row shows the color based handle segmentation by searching within the detected door.

different from that of the door, i.e., the pixel values of the handle should not fall within the (mean + standard deviation) range of the pixel values of the door in grayscale. The detection is done based on a mix of 2D and 3D geometric segmentation techniques explained next.

Fig. 6: Detected door in a fairly complex scene.

Let $P \in R_P$ be a vector containing two vectors P_{2D} and P_{3D} where R_P is the set of all Ps for a particular image. Let $P_{2D} = \begin{bmatrix} u & v \end{bmatrix}^T$ be the pixel coordinates in the 2D image. Let $P_{3D} = \begin{bmatrix} x & y & z \end{bmatrix}^T$ be the coordinates in the 3D task space w.r.t the camera frame for the corresponding 2D image pixel denoted by P_{2D}.

$$P = \begin{bmatrix} P_{2D} & P_{3D} \end{bmatrix}^T \tag{1}$$

Let $P_1, P_2 \in R_P$ belong to detected vertical lines in a 2D image with same v and S_P be a set of $P \in R_P$ where P_{2D} lie in the line joining $P_{1/2D}$ and $P_{2/2D}$. Let D represent a door candidate containing P_1, P_2, S_P. D is given by:

$$D = \begin{bmatrix} P_1 & P_2 & S_P \end{bmatrix}^T \tag{2}$$

For D to belong to a class of DRC doors,

- $\forall P,$ where $P \in S_P,$ and $a,\ b \in \mathbb{R}^3,\ (a - P_{3D}) \cdot b = 0$
- 80 cm $\leq || P_{1/3D} - P_{2/3D} ||_2 \leq 100$ cm

The general idea behind the automatic door detection algorithm is to segment out parallel vertical lines, find the perpendicular distance between them and accept those lines which have a distance of the door width between them.

The first step consists of image filtering. Histogram equalisation is performed to increase the contrast of the image, which facilitates edge detection. Then a bilateral filter is applied to smooth the image. Next, the edges are detected using a Canny edge detector. Lastly, a Probabilistic Hough Transform is applied over the resulting image to find lines.

By checking the line slopes, only the vertical lines which have a pixel length greater than a threshold determined experimentally are kept. Lines are grouped into pairs to form a door candidate. Line pairs that have a pixel distance of less than 60 pixels (also determined experimentally) are also eliminated which reduces the search space but compromises on the detection distance.

At this point the entire image is reprojected in 3D. The line equations for the grouped line pairs are found using RANdom SAmple Consensus (RANSAC). Pairs that have a perpendicular distance of 90 ± 10 cm (90 cm $\equiv$ width of the door) are kept and the rest are discarded. To reduce redundant door pairs due to inaccuracies in line detection, door pairs that have the *same* line equations are merged together. The door pairs are then validated by checking that a solid plane exists in between the two door lines. This is done by taking two diagonals in the door, sampling points on them in the 2D image and checking to see if their 3D counterparts fall on the same plane or not. If not, then the door line pair is rejected, else it is stored as a door. The door plane normal is found by performing a cross product between the line joining the two door edges and any one door edge.

Fig. 7: Handle detection in a complex scene from Fig. 6.

In the second phase of the algorithm handle detection is done based on the assumption that the handle is of a significantly different color than the door:

- The mean (μ) and standard deviation (σ) of the pixels in the image space inside the door region detected earlier are found.

- Connected Component Analysis (CCA) is used to grow the region which corresponds to the pixel value within the range $\mu - \sigma$ and $\mu + \sigma$ and marked as white (see Fig. 7).
- Based on prior knowledge that the handle is on the left or the right hand side, a region is selected correspondingly to exclude the central part of the door.
- In that selected region, the region which is not white starting from the bottom and exceeds a certain contour area threshold ("hard") is selected as the door handle.

Finally, the entire algorithm is repeated over a window of 10 frames. Detections from every frame is recorded. At the end of ten iterations, the detection with the maximum occurrence is selected as the door (Fig. 6 and Fig. 7). Fig. 5 shows the algorithm from different viewpoints.

B. Operator-aided door detection

The general concept for Operator-aided door detection is that the operator supplies a seed either in 3D or in a 2D perspective which is then used to determine the position of the handle and the normal from the door. Our approach has the operator drag the mouse over the latest 2D image from the Robot vision system, marking the position of the handle (see Fig. 8). We refer to each of these 2D operator seeds as scribbles. In this method, the operator scribbles on the door handle and based on the knowledge of where the door handle is, i.e. on the right or on the left of the door, points offset on the side of the seeded point is sampled and a plane is fit to appropriate those points. This provides the handle point (operator seed) and the normal to the door which coupled with the knowledge of the side where the handle gives us the door estimate (see Fig. 9).

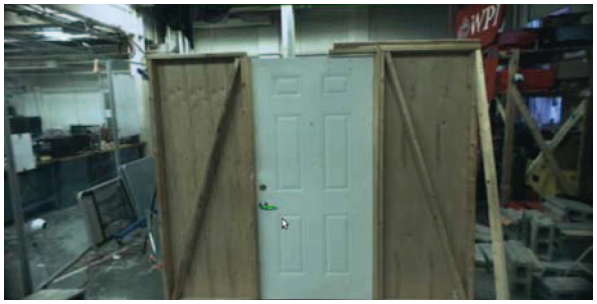

Fig. 8: Operator seed in green color on the handle of the door (near cursor).

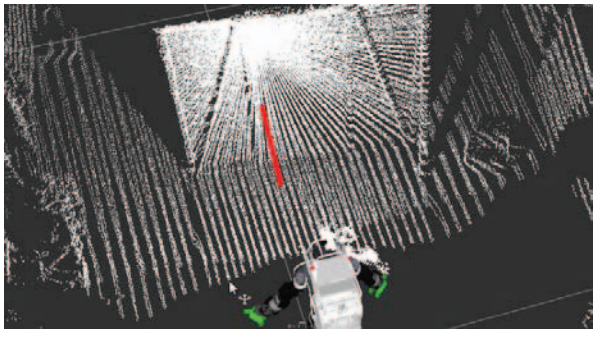

Fig. 9: Detected door normal from the operator seed.

IV. Manipulation - Motion Planning

In order to reliably complete manipulation tasks with a humanoid robot it is important to generate end-effector trajectories that maintain several constraints (like Center of Mass (CoM) over the polygon of support and collision-free motions) simultaneously. One approach is to use a sample-based search algorithm, such as rapidly exploring random trees (RRT) [18] [19] [20], which can efficiently find a feasible path in the search space. This method is probabilistically complete. However, searching in high DoF configuration space and performing post-processing such as smoothing is computationally intensive and time consuming.

Another category is optimization-based algorithms, such as CHOMP [21], STOMP [22] and TrajOpt [23], which can generate a path from an initial trajectory that may be in-collision or dynamically infeasible. The result of the trajectory optimization problem can be obtained in a short period of time, even for a high dimensional problem. But challenges for trajectory optimization are its sensitivity to the choice of initial guesses and getting stuck in local optima.

Since computation time was a high priority consideration in the DRC, and TrajOpt has the best speed performance in the benchmark test compared with other optimization-base algorithms, we decided to adopt a modified TrajOpt as our motion planning library and set up proper costs and constraints for each manipulation task to be performed by our Atlas robot. The way we dealt with the initial guess issue will be described as well.

For the manipulation tasks, the desired Cartesian motions for the robot are specified, such as, foot positions, hand positions and CoM locations. The motion planning optimizer formulates these motions as its costs and constraints, and computes a trajectory represented by the joint states at a set of waypoints. The general formulation of the optimizer is given by:

$$\begin{aligned} \min_{\mathbf{x}} \quad & f(\mathbf{x}) \\ \text{s.t.} \quad & g_i(\mathbf{x}) \geq 0, i = 1,2,...,n_{ieq} \\ & h_j(\mathbf{x}) = 0, j = 1,2,...,n_{eq} \end{aligned} \tag{3}$$

where f , g_i and h_j are scalar functions, n_{ieq} and n_{eq} are the number of the inequality constraints and equality constraints.

In our approach, we consider the robot kinematics only and represent the trajectory as a sequence of T waypoints. The variable $\mathbf{x}$ in (3) is of the form $\mathbf{x} = \mathbf{q}_{1:T}$, where $\mathbf{q}_t \in \Re^K$ describes the joint configuration at the t-th time step for a system with K DoF. The cost function $f(x)$ can be written as:

$$\begin{aligned} f(\mathbf{q}_{1:T}) = \sum_{t=1}^{T} ((\mathbf{q}_{t+1} - \mathbf{q}_t)^T Q_1 (\mathbf{q}_{t+1} - \mathbf{q}_t) + \\ (\mathbf{q}_t - \mathbf{q}_{nom})^T Q_2 (\mathbf{q}_t - \mathbf{q}_{nom}) + \mathbf{d}_\Delta^T Q_3 \mathbf{d}_\Delta) \end{aligned} \tag{4}$$

where $Q1, Q2, Q3$ are weights matrices and have $Q1, Q2$, $Q3 \geq 0$, and $\mathbf{q}_{nom}$ represents a nominal posture. These quadratic cost terms represent penalizations of the weighted sum on the joint displacements between the waypoints, posture deviation from a nominal posture in joint space and

posture error in Cartesian space. The first term can limit the movement of the robot and smooth the trajectory. The second term is used to satisfy desired joint variables when all the constraints have been met. Similarly, the third term is used to push links to specific positions and orientations.

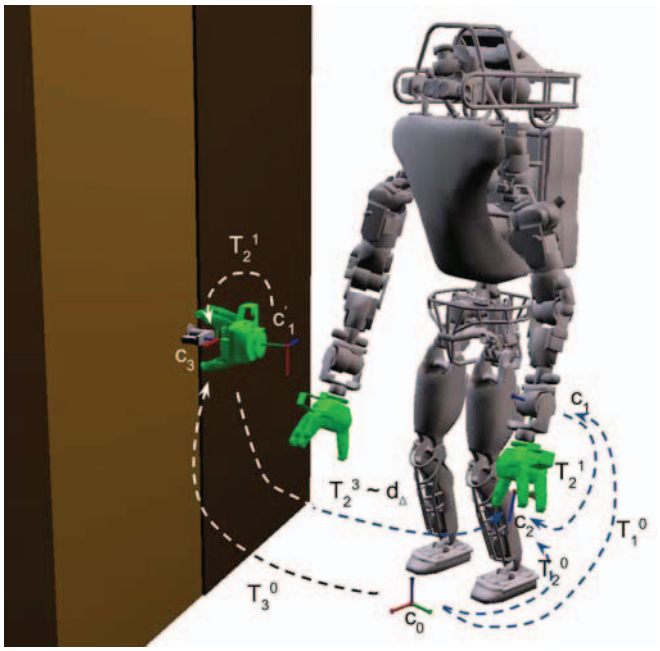

Fig. 10: Transforms and coordinate frames involved in computing the distance $\mathbf{d}_\Delta$. The current end-effector frame is C_1 and the hand pose for grasping handle is C_1'.

The posture error in Cartesian space can be obtained by calculating the distance $\mathbf{d}_\Delta$ from a given configuration to a task space region introduced in [24]. For example, in Fig. 10, the end-effector frame C_1 defined in our Atlas model is on the left wrist. We generate an end-effector frame C_2 for representing the pose of the object held by the hand by setting an offset transform T_2^1. The desired grasp location C_3 is near the door handle. We expect to generate a trajectory that can lead the robot end-effector to reach the desired grasping location. Thus, the distance $\mathbf{d}_\Delta$ means the displacement between C_2 and C_3, which can be computed by converting the transform T_2^3 (5) into a 6×1 displacement vector from the origin of the coordinate of C_3 by (5).

$$T_2^3 = T_0^3 * T_2^0 = (T_3^0)^{-1} * T_1^0 * T_2^1 = \begin{bmatrix} R^{3x3} & t^{3x1} \\ 0 & 1 \end{bmatrix}$$

where R is the rotation matrix and t is the translation vector.

$$\mathbf{d}_\Delta = \begin{bmatrix} t^{3x1} \\ \text{atan2}(R_{32}, R_{33}) \\ -\text{asin}(R_{31}) \\ \text{atan2}(R_{21}, R_{11}) \end{bmatrix} \quad (5)$$

where R_{mn} is an element in the row m and column n.

The constraints for the optimization problem include:

- Joint limits constraint. These can be written as $q - Q^- > 0$, and $Q^+ - q > 0$, where q is the set of reachable joint values, Q^+ is the maximum value in Q, and Q^- is the minimum value.
- Joint posture constraint, which is represented as $q - q_d = 0$. This constraint can lock the joint in some specific value q_d at some time steps.
- Cartesian posture constraint. This constraint can be established by setting the posture error $diag(c_1, c_2, ..., c_6)\mathbf{d}_\Delta = \mathbf{0}$, where $diag(c_1, c_2, ..., c_6)$ is a 6x6 diagonal matrix with diagonal entries from c_1 to c_6. We can relax some position and orientation constraints through setting the related entry to 0.
- CoM constraint. The horizontal projection of the CoM is desired to be on the support convex polygon between two feet. The support polygon can be represented as a intersection of k half planes with the form,

$$a_i x_{CoM} + b_i y_{CoM} + c_i \leq 0, i = 1, 2, 3, ..., k$$

where a_i, b_i, and c_i are scalars. x_{CoM} and y_{CoM} are the location of the CoM projection, which can be computed given the robot posture $\mathbf{q}$.
- Collision avoidance constraint. Generating a collision free trajectory is one of the most important features for the motion planner. But it is difficult to formulate collision constraints in a closed form for the optimization motion planning. We use a hinge-loss function introduced in [23] to set up the collision constraints. The advantage of the method is that it can not only check for discrete collisions in each step but also integrate continuous-time collision avoidance constraints.

Therefore, to generate feasible motion for our Atlas robot, a variety of costs and constraints are set, such as joint displacement costs, knee and back joint nominal value costs, pelvis height and orientation costs, torso orientation costs, shoulder torque costs, joint limit constraints, self-collision constraints, environment collision avoidance constraints, both feet position and orientation constraints, and CoM constraints. These are the general costs and constraints, while according to the requirements of each tasks, some particular costs and constraints also need to be added. For a push door, two trajectories need to be planned, which are approaching the door handle and turning the door handle. For a pull door, the robot also has to pull the door back and block the door from closing with the other hand. The following list describes the specific constraints for each step required to open the door.

1) **Approaching Handle**: A Cartesian posture constraint is added on the final step of the trajectory for approaching the door handle. The parameters of the constraint are the desired position and orientation for the robot end effector to grasp the handle (see Fig. 10), which are computed based on the handle configuration detected by the robot vision system.
2) **Turning Handle**: During the handle turning motion, the handle hinge does not translate. There is only the rotation movement of the hinge. Two Cartesian posture constraints are applied to the trajectory. First is the

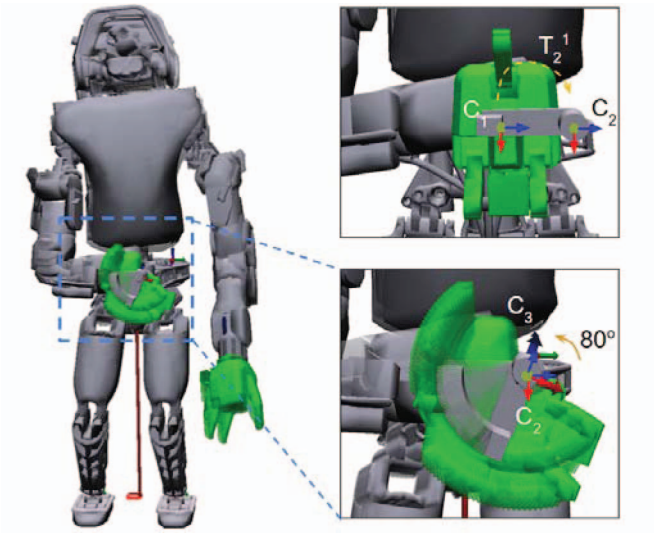

Fig. 11: Constraints on the door handle turning motion plan.

final step constraint. The offset transform T_2^1 is from grasper frame C_1 to the current handle hinge frame C_2, while the target frame C_3 is the current handle hinge frame rotating around 80^o.(see Fig. 11) The second one is a posture constraint for all trajectory steps, which limits the movement of the current handle hinge frame and only allows it to move along the hinge axis through setting the coefficients of the posture constraints $diag(c_1, c_2, ..., c_6)$ as $diag(1,1,1,1,0,1)$. When the handle is held in the hand, the transform T_2^1 can be obtained by adding a minor offset to the current gripper frame configuration, calculated by forward kinematics.

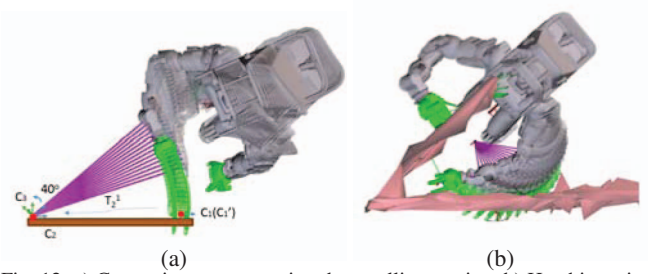

(a) (b)

Fig. 12: a) Constraints on generating door pulling motion. b) Hand insertion trajectory.

3) **Pulling Door Open**: Similar to the handle turning motion, opening the door also has a rotation-only point which is on the door hinge. Hence, the offset transform T_2^1 can be calculated using the width of the door, and the target frame C_3 is the current door hinge frame C_2 rotating around 40^o which is determined experimentally.(see Fig. 12 a) The movement of the current door hinge frame needs to be constrained to be only able to rotate along hinge axis.
4) **Blocking Door from Closing**: After the robot pulls the door out, it needs to insert the other hand to prevent the door from closing again (see Fig. 12 b). There are two Cartesian posture constraints that have to be added. One is positioning the hand grasping the handle during the motion and the other one is moving the other hand to a target position behind the door which can be defined according to the position of the door handle.

Since the optimization problem we formulated involves collision-free constraints which are highly non-convex, the solver may get stuck in infeasible local optima. In our motion planning optimizer, the default method to generate an initial guess is linear interpolation. However, the solver may not be able to obtain a solution from the default initial guess. For example, after pulling out the door using the right hand, the robot needs to insert its left hand to block the door so it will not close again. The environment geometry is generated by convex decomposition [25] of point clouds. (see Fig. 12 b) The initial guess trajectory shows that the left hand has a collision with the wall. In this case, the solver can not find a feasible solution. We use multiple random initializations to help the algorithms escape from the case of local optima. The random initializations can be generated by inserting a random state between the current state and the final desired state and connecting all these states through linear interpolation. Applying this method, the optimizer can find a solution successfully when it is used to generate motions in all DRC scenarios. A disadvantage of using multiple initial guesses is the time cost. To deal with it, we save the computed feasible trajectory and use it as the initial guess next time.

Once the optimization problem is solved, the computed trajectory is sent to our low-level full body controller [26]. The controller traces the trajectory and computes physical quantities for each individual joint such as joint position, velocity, acceleration, and torque. Some of these outputs are then used as references in the joint level servos on the robot.

V. Experiments and Results

In the DRC Finals, the door task was the only task which could not be skipped. Finishing the door task was the only way to be able to attempt the indoor tasks. Hence, it was required that the door task be completed reliably. We started with a pull door to test our perception and motion planning tools. We predicted that opening a pull door would be more difficult than opening a push door because more

TABLE I: Performance of Our Approaches for Both Types of Door

		Door Detection	Walking to the Door	Opening the Door	Walking through the Door	Total
Pull Door	Successful Rate	87.5%	100%	85%	90%	82%
	Time	20.5s	planning step:20.8s moving:41s	an initial guess(4 times):40.4s multiple initial guess:21s moving:111s	124.2s	9min23s
Push Door (Including DRC Finals)	Successful Rate	96%	100%	95%	92%	91%
	Time	19.6s	planning step:13.4s moving:33s	an initial guess(2 times):31s moving:117s	116.5s	7min40s

complex manipulation motions needed to be combined. The test results are shown in Table I Row 2. About a month before DRC Finals, we were informed that there would be a push door in the competition. To switch the strategy from opening a pull door to opening a push door, we just had to change the stand position for opening the door and remove some redundant manipulation motions such as pulling the door open and blocking the door from closing. The results are shown in Table I Row 3. These results include our official runs in the DRC Finals.

Perceiving the location of the door proved to be crucial as the accuracy of stepping and offset parameters depended on it. The door detection results (see Fig. 5 and Fig. 13) (Table II) show that the autonomous door detection performed well with a wide orientation range when the robot was between 1.4 to 2.6 m from the door. The orientation range describes the angle range about the vertical from the ground plane where the robot is standing. For operator aided detection, the orientation ranges were much better and it failed when valid disparity values could not be obtained mostly when the door handle was at the very edge of the image.

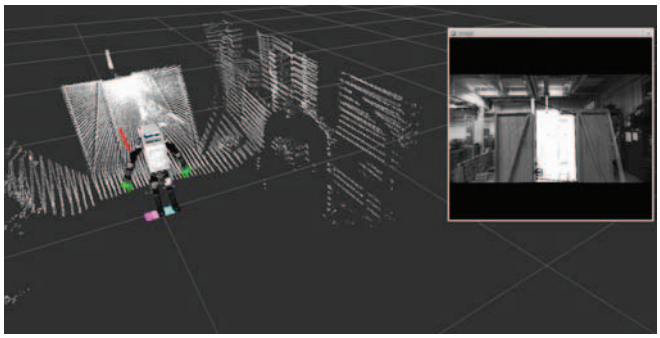

Fig. 13: Door handle detection and its normal visualization.

TABLE II: Door detection results

Autonomous detection			Operator aided detection	
Distance	Orientation (rad)	Result	Orientation (rad)	Result
2.6 - 4 m	-	Failure	-0.5 to 0.6	Success
2.41 - 2.6 m	-0.35 to 0.55	Success	-0.45 to 0.55	Success
1.8 - 2.41 m	-0.2 to 0.5	Success	-0.35 to 0.5	Success
1.4 - 1.8 m	-0.5 to 0.0	Success	-0.5 to 0.45	Success
1.3 m - 1 m	-	Failure	-0.2 to 0.2	Success

Timing and reliability were our highest priority concerns. During the DRC Finals, instead of using autonomous detection techniques we decided to use the operator-aided method for door detection to detect the door handle and the normal. At the Finals, the terrain on which the Atlas walked was not flat and we did not want to lose time in case the autonomous detection failed. At the Finals, the operator scribbled on the door handle in an image getting from Robot vision system and the detection algorithm gave out the handle position and the normal which was then validated by the operator.

Similarly, with motion planning, the operator only needed to confirm the generated trajectory. The average computing time for planning a motion from an initial guess is 10.1 seconds for a pull door and 15.5 seconds for a push door, and from multiple initial guesses it is 21 seconds. The motion

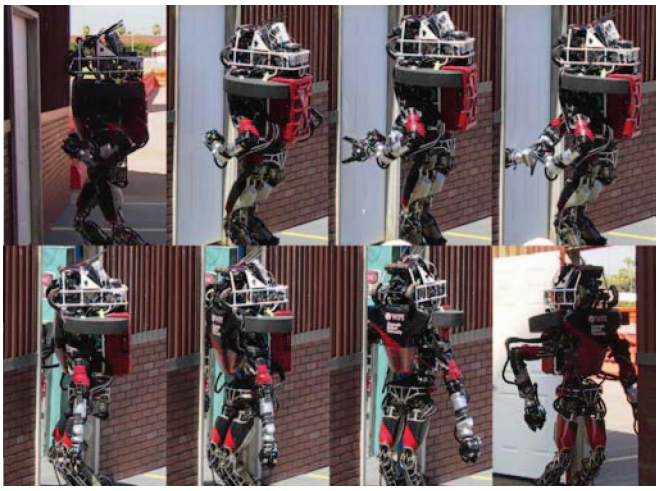

Fig. 14: Door traversal during the DRC Finals

generated from multiple-initial guesses is inserting the other hand to prevent the door from closing again, because the robot had to avoid collision with the complex environment in this motion. For generating motion from multiple-initial guesses, we used a linear interpolated trajectory and two random trajectories as initial guesses in our experiments, and returned the first feasible result coming from our motion planner. The low level controller can precisely trace the generated trajectory. All the failure cases in opening the door were because the hand didn't grasp the handle properly and it slipped off the handle.

VI. Conclusion and Future Work

We have presented our human supervised semi-autonomous approach for executing the door task as stated by the DRC Finals. The door traversal task can be executed reliably in a wide range of unstructured environments with the perception and motion planning algorithms described above showing that shared autonomy works well in solving robotic problems in practice. We successfully completed the door task on both the runs in the DRC Finals (see Fig. 14). We were the only Atlas team that used motion planning to open the door. Other Atlas teams pushed the handle down without grasping it and utilized the self-opening mechanism of the door at the DRC Finals to open it. This hitting motion is very unreliable, and many teams had to try this multiple times at the DRC Finals. Our strategy on the other hand pays a penalty of a little under 20 seconds to finish the motion planning computations and provides a much more robust and reliable door opening motion. In the future, we plan to speed up the motion planner through reuse of previously generated trajectories as initial guesses. Moreover, since our current motion planner only involves kinematic constraints, the low-level controller has to follow the trajectory slowly to avoid dynamic instability. Another area of research would be to introduce key dynamic features into our motion planner so robot trajectory execution can be faster.

ACKNOWLEDGEMENT

This work was sponsored by the Defense Advanced Research Project Agency, DARPA Robotics Challenge Program under Contract No. HR0011-14-C-0011. We also thank Perry Franklin, Benzun Babu and the lab team for their support.

REFERENCES

[1] DARPA, "About the DARPA Robotics Challenge," 2013 2013. [Online]. Available: http://theroboticschallenge.org/about

[2] W. Meeussen, M. Wise, S. Glaser, S. Chitta, C. McGann, P. Mihelich, E. Marder-Eppstein, M. Muja, V. Eruhimov, T. Foote, J. Hsu, R. Rusu, B. Marthi, G. Bradski, K. Konolige, B. Gerkey, and E. Berger, "Autonomous door opening and plugging in with a personal robot," in *Robotics and Automation (ICRA), 2010 IEEE International Conference on*, May 2010, pp. 729–736.

[3] S. Chitta, B. Cohen, and M. Likhachev, "Planning for autonomous door opening with a mobile manipulator," in *Robotics and Automation (ICRA), 2010 IEEE International Conference on*, May 2010, pp. 1799–1806.

[4] B. Axelrod and W. Huang, "Autonomous door opening and traversal," in *Technologies for Practical Robot Applications (TePRA), 2015 IEEE International Conference on*, May 2015, pp. 1–6.

[5] H. Arisumi, N. Kwak, and K. Yokoi, "Systematic touch scheme for a humanoid robot to grasp a door knob," in *Robotics and Automation (ICRA), 2011 IEEE International Conference on*, May 2011, pp. 3324–3331.

[6] M. Prats, P. Sanz, and A. del Pobil, "Reliable non-prehensile door opening through the combination of vision, tactile and force feedback," *Autonomous Robots*, vol. 29, no. 2, pp. 201–218, 2010. [Online]. Available: http://dx.doi.org/10.1007/s10514-010-9192-1

[7] H. Arisumi, J.-R. Chardonnet, and K. Yokoi, "Whole-body motion of a humanoid robot for passing through a door - opening a door by impulsive force -," in *Intelligent Robots and Systems, 2009. IROS 2009. IEEE/RSJ International Conference on*, Oct 2009, pp. 428–434.

[8] M. DeDonato, V. Dimitrov, R. Du, R. Giovacchini, K. Knoedler, X. Long, F. Polido, M. A. Gennert, T. Padr, S. Feng, H. Moriguchi, E. Whitman, X. Xinjilefu, and C. G. Atkeson, "Human-in-the-loop Control of a Humanoid Robot for Disaster Response: A Report from the DARPA Robotics Challenge Trials," *J. Field Robotics*, vol. 32, pp. 275–292, 2015.

[9] M. Zucker, S. Joo, M. X. Grey, C. Rasmussen, E. Huang, M. Stilman, and A. Bobick, "A General-purpose System for Teleoperation of the DRC-HUBO Humanoid Robot," *Journal of Field Robotics*, vol. 32, no. 3, pp. 336–351, 2015. [Online]. Available: http://dx.doi.org/10.1002/rob.21570

[10] S.-J. Yi, S. G. McGill, L. Vadakedathu, Q. He, I. Ha, J. Han, H. Song, M. Rouleau, B.-T. Zhang, D. Hong, M. Yim, and D. D. Lee, "Team THOR's Entry in the DARPA Robotics Challenge Trials 2013," *Journal of Field Robotics*, vol. 32, no. 3, pp. 315–335, 2015. [Online]. Available: http://dx.doi.org/10.1002/rob.21555

[11] M. Johnson, B. Shrewsbury, S. Bertrand, T. Wu, D. Duran, M. Floyd, P. Abeles, D. Stephen, N. Mertins, A. Lesman, J. Carff, W. Rifenburgh, P. Kaveti, W. Straatman, J. Smith, M. Griffioen, B. Layton, T. de Boer, T. Koolen, P. Neuhaus, and J. Pratt, "Team IHMC's Lessons Learned from the DARPA Robotics Challenge Trials," *Journal of Field Robotics*, vol. 32, no. 2, pp. 192–208, 2015. [Online]. Available: http://dx.doi.org/10.1002/rob.21571

[12] M. Fallon, S. Kuindersma, S. Karumanchi, M. Antone, T. Schneider, H. Dai, C. P. D'Arpino, R. Deits, M. DiCicco, D. Fourie, T. Koolen, P. Marion, M. Posa, A. Valenzuela, K.-T. Yu, J. Shah, K. Iagnemma, R. Tedrake, and S. Teller, "An Architecture for Online Affordance-based Perception and Whole-body Planning," *Journal of Field Robotics*, vol. 32, no. 2, pp. 229–254, 2015. [Online]. Available: http://dx.doi.org/10.1002/rob.21546

[13] G. Digioia, H. Arisumi, and K. Yokoi, "Trajectory planner for a humanoid robot passing through a door," in *Humanoid Robots, 2009. Humanoids 2009. 9th IEEE-RAS International Conference on*, Dec 2009, pp. 134–141.

[14] R. B. Rusu, "Semantic 3D Object Maps for Everyday Manipulation in Human Living Environments," *Artificial Intelligence (KI - Kuenstliche Intelligenz)*, 2010 2010.

[15] R. Sekkal, F. Pasteau, M. Babel, B. Brun, and I. Leplumey, "Simple monocular door detection and tracking," in *Image Processing (ICIP), 2013 20th IEEE International Conference on*, Sept 2013, pp. 3929–3933.

[16] W. Shi and J. Samarabandu, "Investigating the Performance of Corridor and Door Detection Algorithms in Different Environments," in *Information and Automation, 2006. ICIA 2006. International Conference on*, Dec 2006, pp. 206–211.

[17] D. Anguelov, D. Koller, E. Parker, and S. Thrun, "Detecting and modeling doors with mobile robots," in *Robotics and Automation, 2004. Proceedings. ICRA '04. 2004 IEEE International Conference on*, vol. 4, April 2004, pp. 3777–3784 Vol.4.

[18] S. M. LaValle, *Planning Algorithms*. Cambridge, U.K.: Cambridge University Press, 2006, available at http://planning.cs.uiuc.edu/.

[19] J. Kuffner and S. LaValle, "RRT-connect: An efficient approach to single-query path planning," in *Robotics and Automation, 2000. Proceedings. ICRA '00. IEEE International Conference on*, vol. 2, 2000, pp. 995–1001 vol.2.

[20] S. Karaman and E. Frazzoli, "Sampling-based Algorithms for Optimal Motion Planning," *International Journal of Robotics Research*, vol. 30, no. 7, pp. 846–894, June 2011.

[21] N. Ratliff, M. Zucker, J. Bagnell, and S. Srinivasa, "CHOMP: Gradient optimization techniques for efficient motion planning," in *Robotics and Automation, 2009. ICRA '09. IEEE International Conference on*, May 2009, pp. 489–494.

[22] M. Kalakrishnan, S. Chitta, E. Theodorou, P. Pastor, and S. Schaal, "STOMP: Stochastic trajectory optimization for motion planning," in *Robotics and Automation (ICRA), 2011 IEEE International Conference on*, May 2011, pp. 4569–4574.

[23] J. Schulman, Y. Duan, J. Ho, A. Lee, I. Awwal, H. Bradlow, J. Pan, S. Patil, K. Goldberg, and P. Abbeel, "Motion planning with sequential convex optimization and convex collision checking," *The International Journal of Robotics Research*, 2014.

[24] D. Berenson, "Constrained Manipulation Planning," Ph.D. dissertation, Robotics Institute, Carnegie Mellon University, Pittsburgh, PA, May 2011.

[25] K. Mamou and F. Ghorbel, "A simple and efficient approach for 3D mesh approximate convex decomposition," in *Image Processing (ICIP), 2009 16th IEEE International Conference on*, Nov 2009, pp. 3501–3504.

[26] S. Feng, E. Whitman, X. Xinjilefu, and C. G. Atkeson, "Optimization-based Full Body Control for the DARPA Robotics Challenge," *Journal of Field Robotics*, vol. 32, no. 2, pp. 293–312, 2015. [Online]. Available: http://dx.doi.org/10.1002/rob.21559